Hepatocyte Nuclear Factor-1β (HNF-1β) Promotes Glucose Uptake and Glycolytic Activity in Ovarian Clear Cell Carcinoma

Takako Okamoto,[1,2] Masaki Mandai,[1]* Noriomi Matsumura,[1] Ken Yamaguchi,[1] Hiroshi Kondoh,[3] Yasuaki Amano,[1] Tsukasa Baba,[1] Junzo Hamanishi,[1] Kaoru Abiko,[1] Kenzo Kosaka,[1] Susan K. Murphy,[2] Seiichi Mori,[4], and Ikuo Konishi[1]

[1]*Department of Gynecology and Obstetrics, Kyoto University Graduate School of Medicine, Kyoto, Japan*
[2]*Department of Obstetrics and Gynecology, Division of Gynecologic Oncology, Duke University Medical Center, Durham, North Carolina*
[3]*Department of Geriatric Medicine, Kyoto University Graduate School of Medicine, Kyoto, Japan*
[4]*Cancer Genomics, Cancer Institute, Japanese Foundation for Cancer Research, Tokyo, Japan*

Ovarian clear cell carcinoma (OCCC) is a morphologically and biologically distinct subtype of ovarian carcinomas that often arises in ovarian endometriosis. We previously reported that a unique carcinogenic environment, especially iron-induced oxidative stress in endometriotic cysts may promote development of OCCC. We also identified a gene expression profile characteristic of OCCC (the "OCCC signature"). This 320-gene OCCC signature is enriched in genes associated with stress response and sugar metabolism. However, the biological implication of this profile is unclear. In this study, we have focused on the biological role of the *HNF-1β* gene within the OCCC signature, which was previously shown to be overexpressed in OCCC. Suppression of HNF-1β in the HNF-1β-overexpressing human ovarian cancer cell line RMG2 using short hairpin RNA resulted in a significant increase in proliferation. It also facilitated glucose uptake, glycolytic activity, and lactate secretion along with increased expression of the glucose transporter-1 (*GLUT-1*) gene and several key enzymes in the glycolytic process. Conversely, forced expression of HNF-1β in the serous ovarian cancer cell line, Hey, resulted in slowed cellular growth and repressed glycolytic activity. These data suggest that HNF-1β represses cell growth, and at the same time, it promotes aerobic glycolysis which is known as the "Warburg effect." As the Warburg effect is regarded as a characteristic metabolic process in cancer which may contribute to cell survival under hypoxic conditions or in a stressful environment, overexpression of HNF-1β may play an inevitable role in the occurrence of OCCC in stressful environment.

Key words: ovarian clear cell carcinoma; HNF1β; glucose metabolism

INTRODUCTION

Ovarian cancer is the leading cause of death among gynecological malignancies. Epithelial ovarian cancer consists of four histologically distinct subtypes, namely, serous, mucinous, endometrioid, and clear cell carcinoma. Ovarian clear cell carcinoma (OCCC) has distinct clinical features as compared to other subtypes: it is generally chemo-resistant, is often accompanied by a thromboembolic complications, and shows slow growth but with unfavorable outcomes. The most notable feature of OCCC is its relationship with ovarian endometriosis. According to epidemiological surveys, approximately 1% of ovarian endometriosis eventually transforms into carcinoma, primarily of the clear cell and endometrioid subtypes. This strongly suggests that there is a specific carcinogenic trajectory that directs the malignant transformation of endometriosis [1–6].

We previously reported that the unique composition of endometriotic cyst fluid, especially the high free iron concentration, promotes carcinogenesis through persistent oxidative stress [7]. We also identified a microarray-based gene signature that is specific to OCCC, which we designated as the "OCCC signature." Analyses of the OCCC signature revealed that OCCC-specific gene expression is characterized by the involvement of many stress-related genes, which further supports the association between OCCC and stress. Pathway analysis of the OCCC signature demonstrated that an intracellular signaling pathway consisting of a large number of genes, especially stress-related genes, is activated in OCCC. A second prominent gene category overrepresented in

Abbreviations: OCCC, ovarian clear cell carcinoma; *HNF-1β*, hepatic nuclear factor-1β gene; shRNA, short hairpin RNAs; qRT-PCR, quantitative real-time polymerase chain reaction; GSEA, gene set enrichment analysis

All the authors have no conflict of interest to declare regarding this manuscript.

*Correspondence to: 54, Kawaharacho, Shogoin, Sakyo ku, Kyoto 606-8507.

Received 15 February 2013; Revised 25 June 2013; Accepted 1 July 2013

DOI 10.1002/mc.22072

Published online in Wiley Online Library (wileyonlinelibrary.com).

the OCCC signature is metabolism-related, in particular glycogen-related genes, suggesting that OCCC has a distinct metabolic character among the ovarian carcinomas [8]. In this context, our next goal was to characterize the genes responsible for this unique expression profile and define the function of these genes, which may then provide the basis for development of targeted molecular therapy that is specific for OCCC. In this study, we have chosen to focus on a specific OCCC signature gene, hepatic nuclear factor-1β gene (*HNF-1β*).

HNF-1β is a homeodomain-containing transcription factor that shares >80% amino acid sequence of homeodomain [9] homology with HNF-1α. These proteins dimerize and bind to the same DNA sequence as homodimers or heterodimers, and are known to regulate the expression of multiple genes through direct or indirect mechanisms [9]. Clinically, *HNF-1* mutations are responsible for "maturity-onset diabetes of the young (MODY)," a specific type of diabetes characterized by pancreatic hypoplasia. Diabetes has been reported in 58% of *HNF-1β* mutation carriers [10]. HNF-1β has been implicated in the development of the pancreas and is thought to be an essential regulator of the transcriptional network that controls pancreatic morphogenesis and the differentiation of pancreatic endocrine cells [11].

Tsuchiya et al. recently reported that HNF-1β is overexpressed in OCCC. Although they identified an anti-apoptotic effect of this gene, the precise mechanism and biological significance of HNF-1β in OCCC are not yet clear [12]. We have shown that HNF-1β is not only a component of the OCCC signature [8], but also included in the intracellular signaling network demonstrated by pathway analysis, suggesting that this gene plays an important role in the biology of OCCC [13]. Therefore, using HNF-1β knockdown in OCCC cells and HNF-1β overexpression in non-OCCC cells, we report herein elucidation of how HNF-1β functionally plays a role in the unique biology of OCCC from multiple point of view including cell proliferation, glucose metabolism and gene expressions.

MATERIALS AND METHODS

Cell Lines and Cell Culture

The OCCC cell lines, RMG1 and RMG2, and the serous carcinoma cell line, Hey, were cultured in RPMI1640 (Nikken, Kyoto, Japan) supplemented with 10% FBS in a humidified atmosphere containing 5% CO_2 at 37°C, as previously described [8].

Stable Knockdown and Overexpression of the *HNF-1β* Gene

Two *HNF-1β*-targeting short hairpin RNAs (shRNA; clone IDs: V2LHS_204881 and V2LHS_196459) and a non-silencing control (clone ID: RHS4348) were purchased from the GIPZ lentiviral shRNAmir library (Thermo Fisher Scientific, Huntsville, AL). RMG2 cells were infected with lentiviruses using a standard protocol using puromycin as the selective marker. RMG2 cells stably transfected with clones V2LHS_204881 or V2LHS_196459 were designated as RMG2-HNFβ-sh1 and RMG2-HNF1β-sh2, respectively, while RMG2 cells transfected with the non-silencing control were designated as RMG2-control. HNF-1β-suppressed stable cells in RMG1 cell line were established using same method above and designated as RMG1-HNF1β-sh1 while non-silencing control cells were designed as RMG1-control. For HNF-1β-overexpressing cell line, an HNF-1β-expressing lentivirus was constructed using an entry vector, pENTR221, containing the HNF-1β cDNA (Cat. No. OHS4559-99857765a; Thermo Fisher Scientific), and a destination vector, pLenti6/V5-DEST, in a Gateway system (Invitrogen Japan, Tokyo, Japan). Hey cells were infected with the HNF-1β-expressing lentivirus and were selected with blasticidin (Hey-HNF1β). The Hey cells transfected with an empty lentiviral vector were used as a control (Hey-control).

RNA Extraction and Quantitative Real-Time Polymerase Chain Reaction (qRT-PCR)

Total RNA was isolated from cells at 80% confluency using the RNeasy Mini Kit (Qiagen, Tokyo, Japan). Quantitative RT-PCR (qRT-PCR) was performed with primers and probe specific for *HNF-1β* (Assay ID: Hs00172123_ml) and *SOD1* (Assay ID: Hs00533490_m1; Taqman Gene Expression Assays; Applied Biosystems, Foster City, CA). All other assays were designed using Roche Probefinder software at the Universal Probe Library Assay Design Center (https://www.roche-applied-science.com/sis/rtpcr/upl/index.jsp?id=UP030000). Primer and probe sequences are provided in Supplementary Table 1. The samples were analyzed using a LightCycler 480 Real-Time PCR system (Roche Diagnostics, Tokyo, Japan).

Protein Extraction and Western Blot Analysis

Protein extraction and Western blotting were performed as reported previously [13] using the following primary antibodies: anti-HNF-1β (1:200; Santa Cruz, CA), anti-CDKN1B (1:1000, BD Bioscience, Franklin Lakes, NJ), anti-CDKN1A (1:200; Santa Cruz, CA), anti-GLUT1 (1:2500, Abcam Plc, Cambridge, UK), and anti-β-Actin (1:5000, Abcam Plc). Horseradish peroxidase-linked secondary antibodies were as follows: anti-goat Ig for HNF-1β (1:10 000, DAKO, Glostrup, Denmark) and CDKN1A (1:3000, GE Healthcare, Buckinghamshire, UK), anti-mouse Ig for CDKN1B (1:1000, GE Healthcare) and GAPDH (1:1000, Santa Cruz, CA), anti-rabbit Ig for GLUT1 and β-actin (1:2500 and 1:10 000, respectively, GE Healthcare). Images were obtained using a ChemiDoc XRS Plus system (Bio-Rad Laboratories, Tokyo, Japan).

Proliferation Assays

Cells were seeded into 96-well (2.5×10^3 cells/well) tissue culture plates and incubated for 3 d. Cell numbers were counted at three consecutive time points using a WST-8 (Water Soluble Tetrazolium salts) assay kit, which is a modified MTT (3-(4,5-di-methylthiazol-2-yl)-2,5-diphenyltetrazolium bromide) assay (Nakalai tesque, Kyoto, Japan). WST-8 assay values were normalized using the WST-8 value at the initial time point (Day 0), and compared between the groups. Population doubling times (PDT) were calculated based on the slope angle of the linear regression model for the three time points. In addition to WST-8 assays, cell numbers were directly counted in sextuplicate using the Countess Automated cell counter (Invitrogen) after the cells were seeded into 6-well tissue culture plates (3.0×10^5 cells/well) and incubated for 2, 5, and 11 d. The values were normalized at the initial time point (Day 0) same as above.

The Cell Cycle Analysis

The cell cycle analysis was performed as described previously [14]. The cells (1×10^6/well) were seeded in 10 cm^2 tissue culture dishes and cultured. The next day, cells were treated by nocodazole (Sigma–Aldrich, St. Louis, MO) at a final concentration of 0.5 μg/mL. After incubation for 0, 12, 24 h, cells were fixed with 70% ethanol, stained with 25 μg/mL propidium iodide (Sigma–Aldrich) and analyzed by FACS-Calibur flow cytometry with Cell Quest software (Becton Dickson, Franklin Lakes, NJ). For analysis of S-phase cell, cells were pulse-labeled with 10 μM BrdU for 1 h, fixed with 70% ethanol, denatured, and stained with APC conjugated Anti-BrdU Antibody (Becton Dickson), according to manufacturer's instructions.

Glucose Uptake Assay and Measurement of Lactate Production

Glucose uptake assays were performed as reported previously [15]. In brief, cells were incubated with glucose-free medium with 1 μCi 2-deoxy-[^{3}H]-D-glucose for 60 min. The cells were then washed three times with ice-cold PBS, collected, and quantified using a liquid scintillation counter. Lactate production was evaluated by measuring the concentration in the medium after 24 h of incubation. The assay was performed in triplicate, repeated three times and all the values were normalized by total protein concentration.

Glycolytic Flux Measurement

Measurement of glycolytic flux was performed as reported previously [16]. In brief, $0.7–3.0 \times 10^6$ cells were plated in a 10 cm^2 dish. The medium was changed the following day to a low-glucose (4.25 mmol/L) medium, and 12 h later, D-[3-^{3}H] glucose (3.6 μCi) was added. Every 2 h, 400 μL of the medium was taken for perchloric acid precipitation. The supernatant was applied to DOWEX 1×8 200–400 MESH Cl resin (Sigma–Aldrich Japan) after dilution in sodium tetraborate. The assay was performed in triplicate, repeated three times and the values were normalized by total protein concentration.

Glucose Uptake After Knockdown of GLUT1 in RMG2 Cells

GLUT1-specific siRNAs (Gene Solution siRNA, Cat. No. SI03089401 and No. SI00089264; Qiagen, Valencia, CA) and a negative-control siRNA (AllStars Negative Control siRNA; Qiagen) were transfected into RMG2 cells using HiPerFect Transfection Reagent (Qiagen). After 48 h incubation for with the siRNAs, glucose uptake assays were performed as described above. To confirm downregulation of *GLUT1* expression, qRT-PCR and Western blotting were performed as described above.

Microarray Analysis

RNA preparation and microarray analysis were performed as described [8,13]. Genome set Human U133 Plus 2.0 chips (Affymetrix, Santa Clara, CA) were used and expression of HNF-1β-knockdown and non-silencing control cells were compared using replicate cell preparations (five replicates each for RMG2-HNF1β-sh1 and RMG2-HNF1β-sh2, ten replicates for the RMG2-control). The enrichment of the OCCC signature in control (non-silencing) cells versus HNF-1β-knockdown cells was evaluated using Gene Set Enrichment Analysis (http://www.broadinstitute.org/gsea/index.jsp; GSEA). GSEA is a tool to determine if a particular set of pre-defined genes is over- or under-represented in a given sample. Here, probe sets that were previously shown [8] to be upregulated ($n = 393$) and downregulated ($n = 44$) were analyzed in RMG2 cells following knockdown of HNF-1β using two independent shRNAs. Interpretation of output figures is described in detail in the GSEA website (http://www.broadinstitute.org/gsea/index.jsp). Bayesian binary regression 2.0 (http://data.genome.duke.edu/oncogene.php) was used to calculate the HNF-1β signature probability scores of cells, indicating transcriptional pathway activity of HNF-1β downstream genes. Published microarray dataset GSE6008 (consisting of data from 8 OCCC and 91 non-OCCC specimens) was obtained from the Gene Expression Omnibus (GEO) website (http://www.ncbi.nlm.nih.gov/geo/). The GSE2109 dataset was also obtained from the GEO website, and 16 OCCC and 184 non-OCCC (excluding borderline tumors) were used for this analysis. Cell lines used in the present study are listed in Supplementary Table 2.

Statistical Analysis

Differences between groups were assessed using two-tailed unpaired *t*-tests. Data are represented

as mean ± standard deviation (SD). Statistical analysis was performed using GraphPad Prism 4 software (GraphPad Software, Inc., La Jolla, CA), and probability values below 0.05 were considered as significant.

RESULTS

Effect of HNF-1β Knockdown on In Vitro Cell Proliferation

Expression of *HNF-1β* mRNA in shRNA-transfected cells was evaluated using qRT-PCR. *HNF-1β* expression was significantly suppressed (% suppression is 87.3% in RMG2-HNF1β-sh1 ($P = 0.009$) and 71.6% in RMG2-HNF1β-sh2 ($P = 0.013$) compared with the RMG2-control cells (Figure 1A). Suppression of HNF-1β protein was also confirmed by Western blot (Figure 1A).

Silencing of HNF-1β was associated with an increase in cell proliferation in RMG2 cells as detected using WST-8 assays ($P < 0.01$; Figure 1B) and based on cell counts ($P < 0.0001$; Figure 1B). PDT of RMG2-HNF1β-sh1, RMG2-HNF1β-sh2, and RMG2-control cells were 27.2, 21.5, and 34.5 h, respectively, as assessed by WST-8 assays, and were 1.94, 1.43, and 2.37 d, respectively, based on direct cell counts.

The suppression of HNF-1β in another OCCC cells, RMG1 (% suppression was 72.8% in RMG1-HNF1β-sh1 ($P = 0.041$; Figure 2A)) also caused accelerated cell proliferation as compared to control cells ($P < 0.0001$; Figure 2B). PDT of RMG1-HNF1β-sh1 and RMG1-control cells by WST-8 assays were 41.9 and 65.2 h, respectively.

Effect of HNF-1β Knockdown on Cell Cycle Progression and the Expression of CDKN1A and CDKN1B

We evaluated cell cycle progression by using Nocodazole, which arrests cell cycle at G2/M phase. Non-silencing RMG2 cells were significantly retarded in the transition G1/S to G2/M phase after 12, 24 h incubation with Nocodazole, compared to HNF-1β-knockdown RMG2 cells (Figure 1C). In addition, the detection of BrdU incorporation revealed that the percentage of S-phase cell was significantly reduced in 19.9% in RMG2-control cells, compared with 29.1% in RMG2-HNF1β-sh1 and 28.9% in RMG2-HNF1β-sh2 (Figure 1D).

Since HNF-1β knockdown resulted in an increase in cell proliferation in RMG2 cells, we evaluated CDKN1A and CDKN1B expression in HNF-1β-knockdown and non-silencing RMG2 cells by Western blot. CDKN1B protein levels in both RMG2-HNF1β-sh1 and RMG2-HNF1β-sh2 were significantly repressed as compared with the RMG2-control cells (% suppressions were 61.9% and 81.8%, respectively; Figure 1E). CDKN1A protein levels were also suppressed in RMG2-HNF1β-knockdown cells compared with RMG2-control cells (% suppressions were 81.9% and 83.1%, respectively; Figure 1F).

Effect of HNF-1β Knockdown on Glucose Uptake, Glycolytic Flux, and Lactate Secretion

The rate of glucose uptake was measured using a scintillation counter and normalized to that of non-silencing control cells. Uptake of extracellular glucose was significantly decreased in HNF-1β-knockdown cells as compared to control cells (RMG2-HNF1β-sh1, $42.6 \pm 6.56\%$, $P = 0.0019$; RMG2-HNF1β-sh2, $40.2 \pm 5.29\%$ $P = 0.0014$; Figure 3A).

To verify that HNF-1β promotes glycolytic activity, we further examined glycolytic flux, which was determined by measuring the rate per hour of conversion of ^{3}H-labeled glucose to H_2O through the glycolytic pathway (Figure 3B). Glycolytic flux was significantly decreased in HNF-1β-knockdown cells as compared to control cells (RMG2-HNF1β-sh1, $56.0 \pm 8.78\%$, $P = 0.0012$; RMG2-HNF1β-sh2, $49.8 \pm 2.56\%$, $P < 0.0001$; Figure 3B).

Lactate secretion into the culture media was also measured and was significantly suppressed in HNF-1β-knockdown cells (RMG2-HNF1β-sh1, $70.0 \pm 6.46\%$, $P = 0.030$ and RMG2-HNF1β-sh2, $45.2 \pm 8.53\%$, $P = 0.0047$) relative to the control cells (Figure 3C).

We also analyzed the effect of HNF-1β on glucose metabolism using another OCCC cell line, RMG1. Glucose uptake ($69.0 \pm 1.60\%$, $P = 0.0008$; Figure 3D), glycolytic flux ($71.5 \pm 1.35\%$, $P = 0.0003$; Figure 3E) and lactic acid production ($60.0 \pm 0.98\%$, $P < 0.0001$; Figure 3F) in RMG1-HNF1β-sh1 cells were also significantly suppressed compared to control cells.

Effect of HNF-1β Overexpression on Cell Proliferation, Glucose Uptake, Glycolytic Flux, and Lactate Secretion

Expression of HNF-1β was determined by qRT-PCR and Western blot following transfection of the *HNF-1β* gene construct into Hey ovarian cancer cells. Both the mRNA and protein levels were markedly increased in Hey-HNF1β compared with the Hey-control cells (Figure 2A). Forced expression of HNF-1β in Hey cells led to a decrease in cell proliferation, as measured using the WST-8 assay ($P = 0.0003$; Figure 2B). The PDT of Hey-control and Hey-HNF1β was 11.9 and 14.9 h, respectively.

Glucose uptake was significantly increased in Hey-HNF1β cells when compared with Hey-control cells ($231 \pm 65.2\%$ vs. $100 \pm 28.8\%$, $P = 0.0334$; Figure 3G). Hey-HNF1β cells also exhibited enhanced glycolytic flux relative to the Hey-control cells ($120 \pm 7.26\%$ vs. $100 \pm 2.84\%$, $P = 0.0099$; Figure 3H).

Lactate production over the course of 24 h was also elevated in Hey-HNF1β cells compared with that in Hey-control cells ($118 \pm 7.74\%$ vs. $100 \pm 8.37\%$, $P = 0.0028$; Figure 3I).

Moreover, forced expression of HNF-1β in the immortalized human ovarian surface cell line (HOSE/E7/hTERT) showed a similar result as Hey

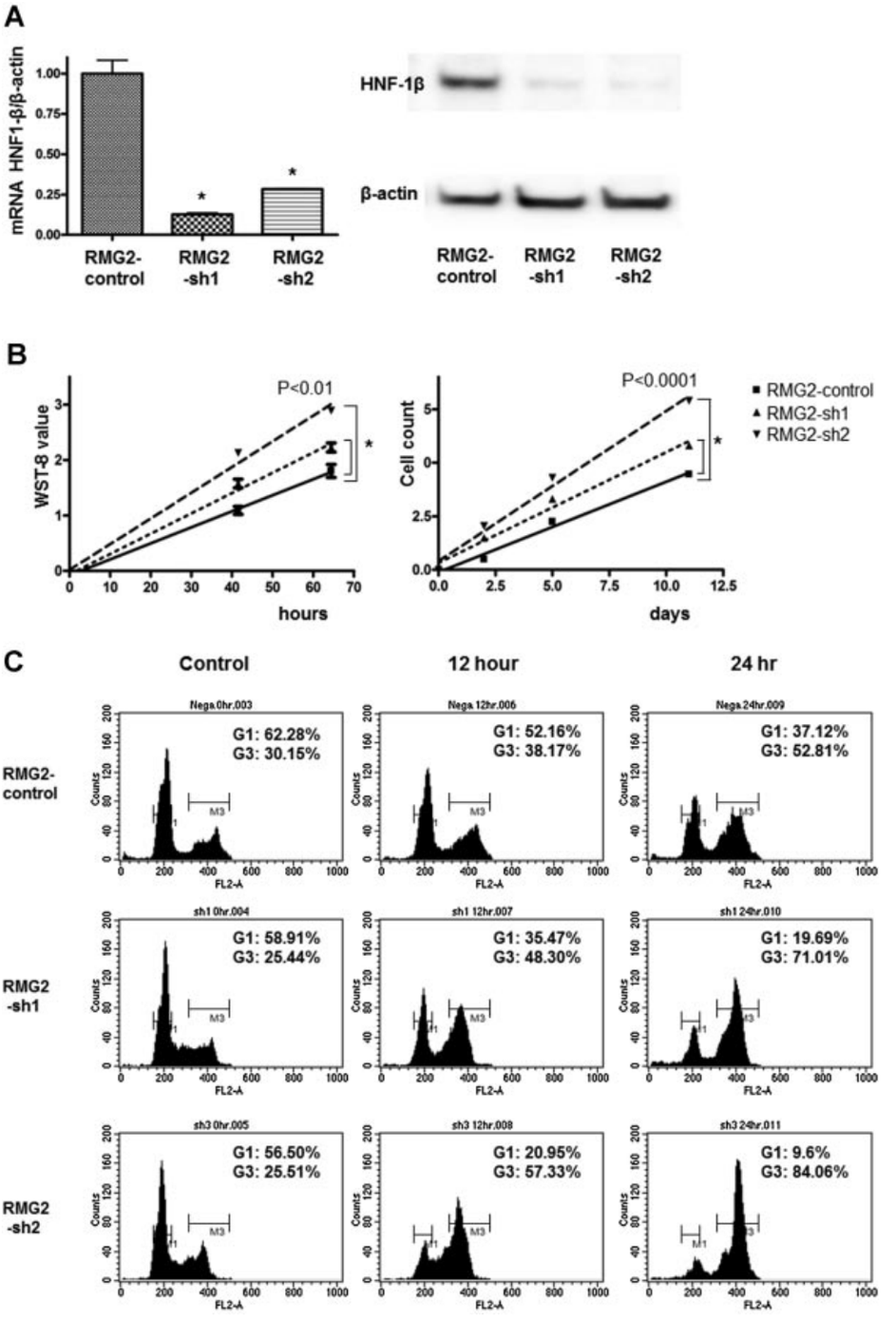

Figure 1. Short hairpin RNA mediated knockdown of HNF-1β expression enhanced cell proliferation rates with suppression of CDKN1A and CDKN1B protein expression and progressed cell cycle the G1/S to G2/M phase. (A) *HNF-1β* mRNA expression detected by quantitative RT-PCR (left panel). HNF-1β protein expression detected by Western blot analysis (right panel). (B) Cell proliferation curve produced from results of the WST-8 assay (left panel). Cell proliferation curve produced by direct cell counts (right panel). *x*-axis, incubation time; *y*-axis, relative number cells in $\log_2$ scale. In detail, relative number cells are determined as WST-8 value (number of cells) divided by WST-8 (number of cells) value at 0 h (0 d). (C) Cell cycle analysis using PI after 12, 24 h nocodazole treatment. (D) The cell cycle analysis using BrdU incorporation. (E) CDKN1B protein expression by Western blot analysis. (F) CDKN1A protein expression by Western blot analysis. The right panels of (E) and (F) showed the quantified protein expressions which were normalized with the expression in control cells. RMG2-sh1, RMG2-HNF1β-sh1; RMG2-sh2, RMG2-HNF1β-sh2; G1, G1 phase; G3, G3 phase; $^*P < 0.01$.

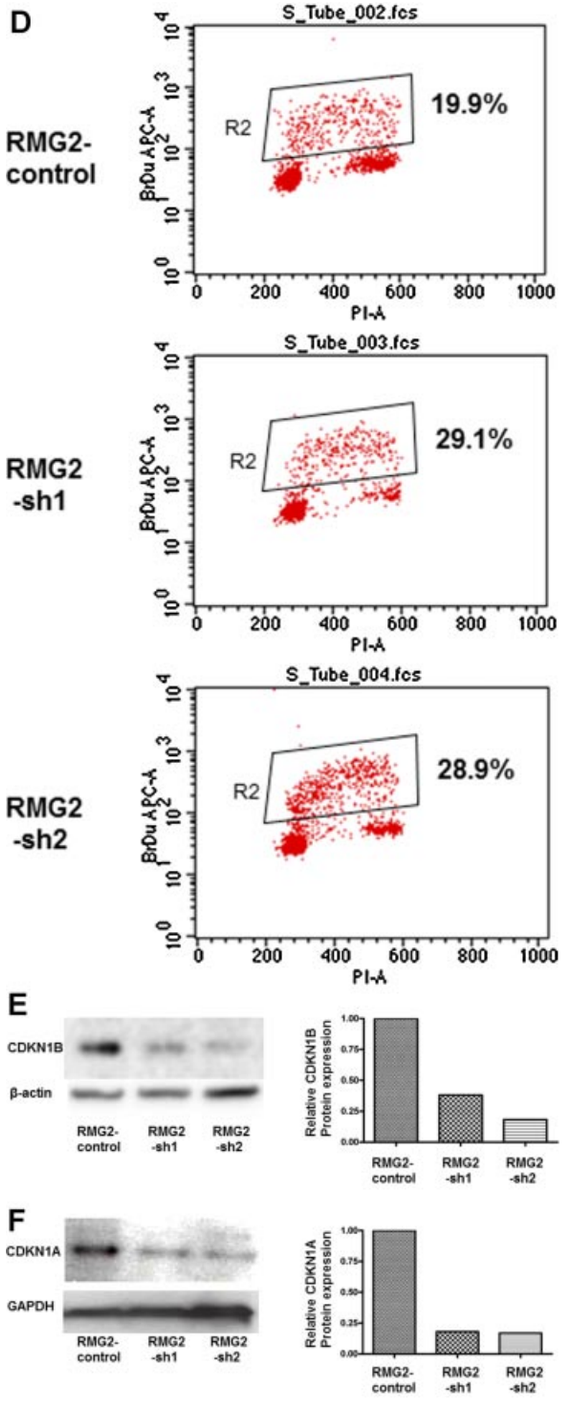

Figure 1. (*Continued*)

cell in glucose uptake, glycolytic flux and lactate production (Supplementary Figure 2).

Effect of HNF-1β Knockdown and Overexpression on GLUT1 Expression

GLUT1 mRNA expression in HNF-1β-knockdown RMG2 cells was evaluated by qRT-PCR and found to be repressed as compared to the control cells (RMG2-HNF1β-sh1, $36.3 \pm 0.19\%$, $P = 0.0001$ and RMG2-HNF1β-sh2, $40.5 \pm 0.20\%$, $P = 0.0001$; Figure 4A). Likewise, the expression of GLUT1 protein was also lower in the HNF-1β-knockdown cells than that observed in the non-silencing control cells (Figure 4B). In addition, the mRNA expression of *GLUT1* in RMG1-HNF1β-sh1 was also decreased as compared to control cells ($84.94\% \pm 1.25\%$, $P = 0.035$; Figure 4C). GLUT1 protein expression was also suppressed in RMG1-HNF1β-sh1 (Figure 4D).

Inversely, the expression of *GLUT1* mRNA in Hey-HNF1β cells was more than 2-fold higher than that in Hey-control cells ($228 \pm 11.2\%$ vs. $100 \pm 0.98\%$, $P = 0.0073$; Figure 4E). GLUT1 protein expression was also elevated in the HNF-1β-overexpressing cells (Figure 4F).

Effect of HNF-1β Suppression on Glycolytic Enzymes and HIF-1α Expression

Messenger RNA expression levels of most of the glycolytic enzymes (Hexokinase1 (*HK1*), Hexokinase2 (*HK2*), Glucose-6-phosphate isomerase (*GPI*), Phosphofructokinase liver type (*PFK-L*), Phosphofructokinase platelet type (*PFK-P*), Aldolase A (*ALDOA*), Aldolase B (*ALDOB*), Aldolase C (*ALDOC*), Triosephosphate isomerase (*TPI*), Phosphoglycerate kinase 1 (*PGK1*), Phosphoglycerate kinase 2 (*PGK2*), Phosphoglycerate mutase 1 (*PGAM1*), Enolase 2 (*ENO2*), Enolase 3 (*ENO3*), Lactose dehydrogenase A (*LDHA*), Lactose dehydrogenase B (*LDHB*)) were significantly decreased in RMG2-HNF1β-sh1 cells as compared with the RMG2-control group (Figure 5).

Since HIF-1α is implicated in the stress-resistance in several cell lines, we examined if HNF-1β affects HIF-1α expression. Expression levels of *HIF-1α* mRNA were not significantly different between RMG2-HNF1β-sh1, RMG2-HNF1β-sh2, and RMG2-control cells (Supplementary Figure 3).

Effect of HNF-1β Suppression on OCCC Signature

OCCC signature upregulated genes (393 probe sets) were significantly enriched in the non-silencing control cell group as compared with the HNF-1β-knockdown cells (RMG2-HNF1β-sh1, RMG2-HNF1β-sh2; FDRq-value < 0.0001 and < 0.0001, respectively; Figure 6A). OCCC signature downregulated genes (44 probe sets) were significantly enriched in the HNF-1β-knockdown cells when compared with the non-silencing control cells (FDRq-value $= 0.0019$ and 0.0051, respectively; Figure 6B). These data indicate that by suppressing HNF-1β activity, the OCCC signature profile is altered in a manner that more closely matches the non-OCCC gene signature profile.

Creation of an HNF-1β Signature From HNF-1β-knockdown Microarray Data

We analyzed the gene expression microarray data derived from the HNF-1β-knockdown cells and the

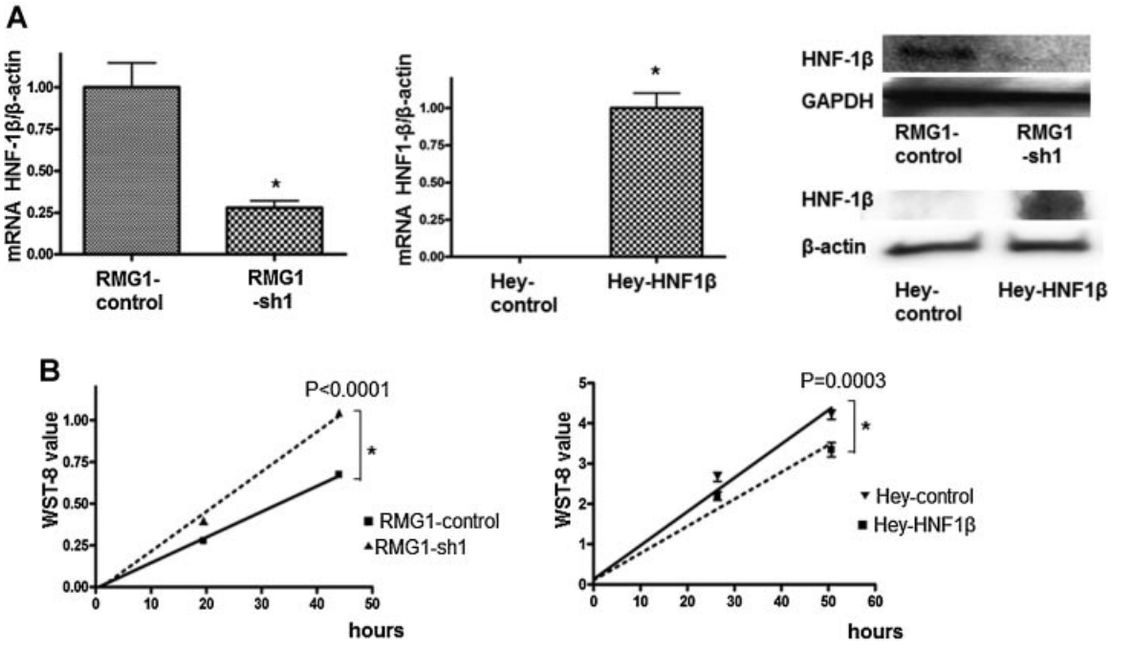

Figure 2. Knockdown of HNF-1β in RMG1 cells and forced expression of HNF-1β in Hey cells also affected the cell proliferation rate. (A) *HNF-1β* mRNA expression detected by quantitative RT-PCR (left and central panel). HNF-1β protein expression by Western blot analysis (right panel). (B) Cell proliferation curve produced from results of the WST-8 assay. RMG1-sh1, RMG1-HNF1β-sh1; $^*P < 0.05$. Experiments were done three times in triplicate.

non-silencing control cells using Bayesian binary regression 2.0, and derived an HNF-1β signature that consists of 250 probe sets (Supplementary Table 3) that are differentially expressed between these two groups (Figure 6C and D). The HNF-1β signature was able to distinguish OCCC from non-OCCC in the clinical ovarian cancer dataset GSE6008 (HNF-1β signature probability, 0.934 ± 0.0378 in OCCC vs. 0.423 ± 0.208 in non-OCCC, $P < 0.0001$) and in dataset GSE2109 (HNF-1β signature probability, 0.632 ± 0.297 in OCCC vs. 0.478 ± 0.224 in non-OCCC, $P = 0.0112$), as well as in the ovarian cancer cell line dataset KyotoOv [8] (HNF-1β signature probability, 0.610 ± 0.196 in OCCC vs.0.409 ± 0.221 in non-OCCC, $P = 0.012$; Figure 6D).

Effect of GLUT1 Knockdown on Glucose Uptake of RMG2 Cells

Knockdown of GLUT1 was performed using *GLUT1*-specific siRNAs (siRNA1, siRNA2). Over 41.8% (siRNA1) and 49.6% (siRNA2) knockdown of *GLUT1* expression was achieved as measured by qRT-PCR and 87.7% (siRNA1) and 61.7% (siRNA2) reduction in GLUT1 protein levels measured by Western blot (Supplementary Figure 1A and B). Glucose uptake following GLUT1 suppression was decreased relative to that observed in the cells receiving the negative-control siRNA (siRNA1, $73.7 \pm 7.72\%$, $P = 0.0074$; siRNA2, $70.8 \pm 6.28\%$, $P = 0.0030$; Supplementary Figure 1C).

Effect of HNF-1β Suppression on the Expression of Superoxide Dismutase 1 (*SOD1*)

In the microarray data derived from the HNF-1β-knockdown cells and the non-silencing control cells, the expression of *SOD1*, which is one of oxidative stress genes, were significantly suppressed in RMG2-HNF1β-sh1 cells ($P < 0.0001$) and RMG2-HNF1β-sh2 cells ($P = 0.0002$) as compared with the RMG2-control (Figure 6F).

Further, we validated the *SOD1* mRNA expression by using qRT-PCR. The expression was significantly decreased in RMG2-HNF1β-sh1 cells ($P = 0.0012$) and RMG2-HNF1β-sh2 cells ($P = 0.0001$) as compared with the RMG2-control (Figure 6G). Using another OCCC cell line, RMG1, HNF-1β suppression also caused decrease in mRNA expression of *SOD1* genes ($P = 0.029$; Figure 6G).

The expression of Glutathione peroxidase (*GPX*), which is also one of the oxidative stress genes, was also decreased in HNF-1β-suppressed cells (Supplementary Figure 4).

DISCUSSION

We previously identified an OCCC-specific gene expression signature that contains multiple genes with functional relevance to the biology of clear cell carcinomas, including *HIF-1α*, *IL-6*, and *HNF-1β*. In this study, we focused on the role of HNF-1β in OCCC for several reasons. First, HNF-1β is overexpressed

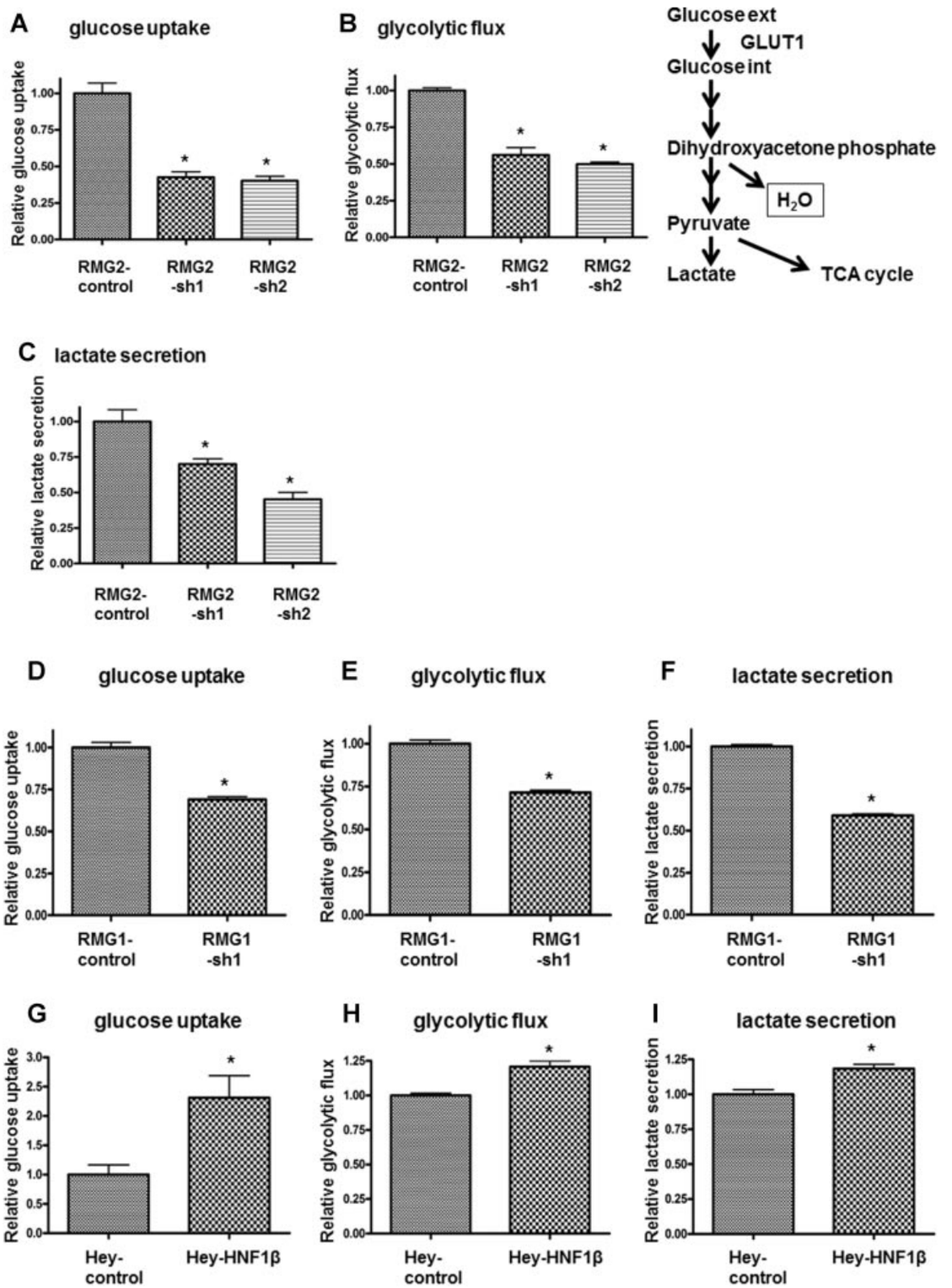

Figure 3. Knockdown of HNF-1β in RMG2 and RMG1 cells was associated with the decrease of glucose uptake, glycolytic flux, and lactate secretion. Conversely, forced expression of HNF-1β in Hey cells was associated with the increase of them. (A) Glucose uptake in RMG2 cells. (B) Glycolytic flux in RMG2 cells (left panel). Scheme of simplified glycolytic pathway (right panel). (C) Lactate secretion in RMG2 cells. (D) Glucose uptake in RMG1 cells. (E) Glycolytic flux in RMG1 cells. (F) Lactate secretion in RMG1 cells. (G) Glucose uptake in Hey cells. (H) Glycolytic flux in Hey cells. (I) Lactate secretion in Hey cells. RMG2-sh1, RMG2-HNF1β-sh1; RMG2-sh2, RMG2-HNF1β-sh2; RMG1-sh1, RMG1-HNF1β-sh1. $^{*}P < 0.05$.

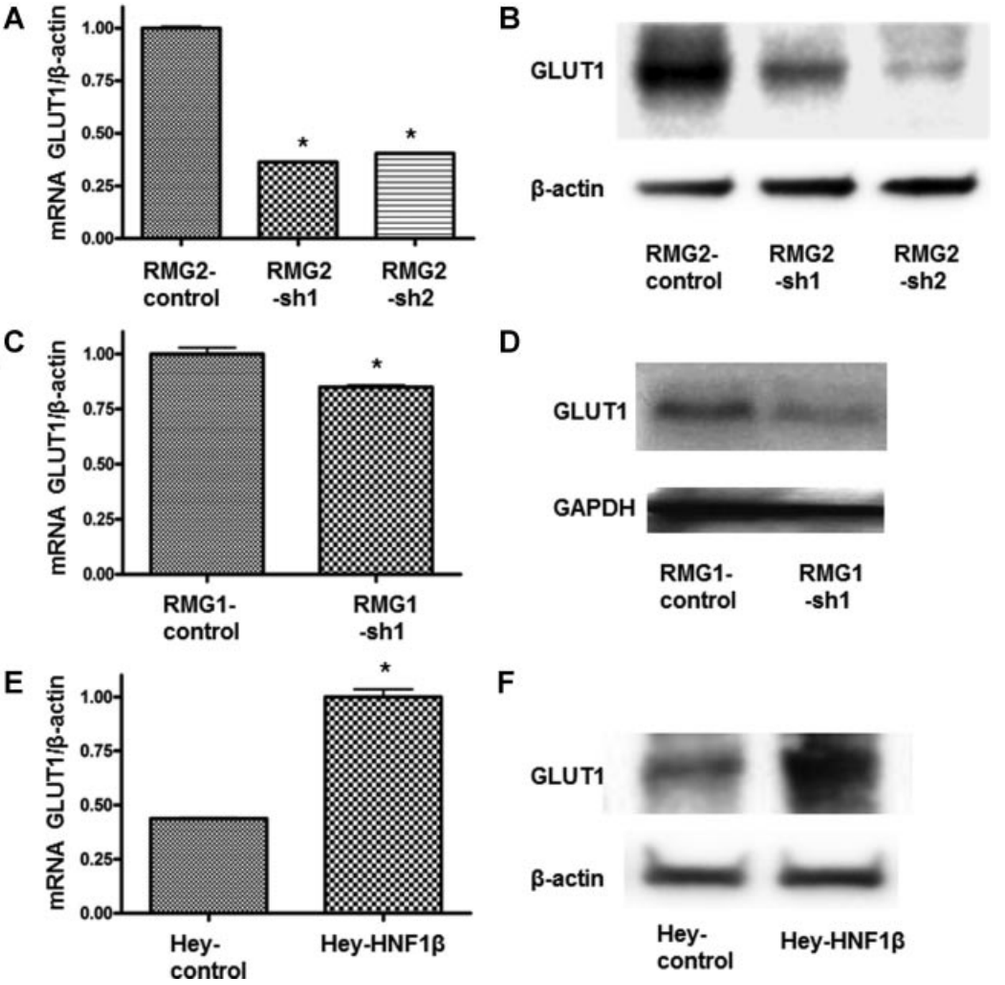

Figure 4. HNF-1β upregulated GLUT1 expression. Knockdown of HNF-1β expression in RMG2 suppressed *GLUT1* mRNA (A) and protein (B). Knockdown of HNF-1β expression in RMG1 suppressed *GLUT1* mRNA (C) and protein expression (D). Forced expression of HNF-1β in Hey cells increased *GLUT1* mRNA (E) and protein expression (F). RMG2-sh1, RMG2-HNF1β-sh1; RMG2-sh2, RMG2-HNF1β-sh2; RMG1-sh1, RMG1-HNF1β-sh1. $^*P < 0.05$.

specifically in the clear cell histologic type of epithelial ovarian cancer [12,17–19], which we also confirmed by gene expression microarray and RT-PCR [8]. Second, we have shown that the expression of HNF-1β is epigenetically regulated [8,20], which is an important and pharmacologically reversible feature of many cancer-associated genes. Third, activation of the HNF-1β signaling network was strongly predicted from the pathway analysis of the OCCC signature, indicating that HNF-1β is a central mediator of the OCCC-specific signaling network [8,13]. Finally, transcription factor binding motif analysis showed that HNF-1β binding motifs are significantly enriched among genes that comprise the OCCC signature [13]. Taken together, these findings strongly suggested that HNF-1β plays a central role in the manifestation of the unique biological phenotype of OCCC, but the mechanisms driving this have been thus far unclear.

To begin a functional analysis of HNF-1β in OCCC, we chose to use RMG2, a human OCCC cell line, because it phenotypically resembles clinical OCCC and is also thought to be best representative of OCCC from the context of gene expression profiles as measured by microarray analyses. Knockdown of HNF-1β expression in RMG2 cells using lentiviral transfer of gene-specific shRNAs resulted in a marked shift in the OCCC signature toward a non-OCCC gene expression profile, suggesting that, as predicted, HNF-1β is a key molecule in maintaining an OCCC biological phenotype (Figure 6A and B). To confirm the significance of HNF-1β in OCCC, we also used binary regression 2.0 to develop an HNF-1β gene signature using gene expression microarray data obtained from HNF-1β-knockdown and control cells. The HNF-1β gene signature consists of the group of genes that are differentially expressed between the HNF-1β-knockdown and control RMG2 cells, and has

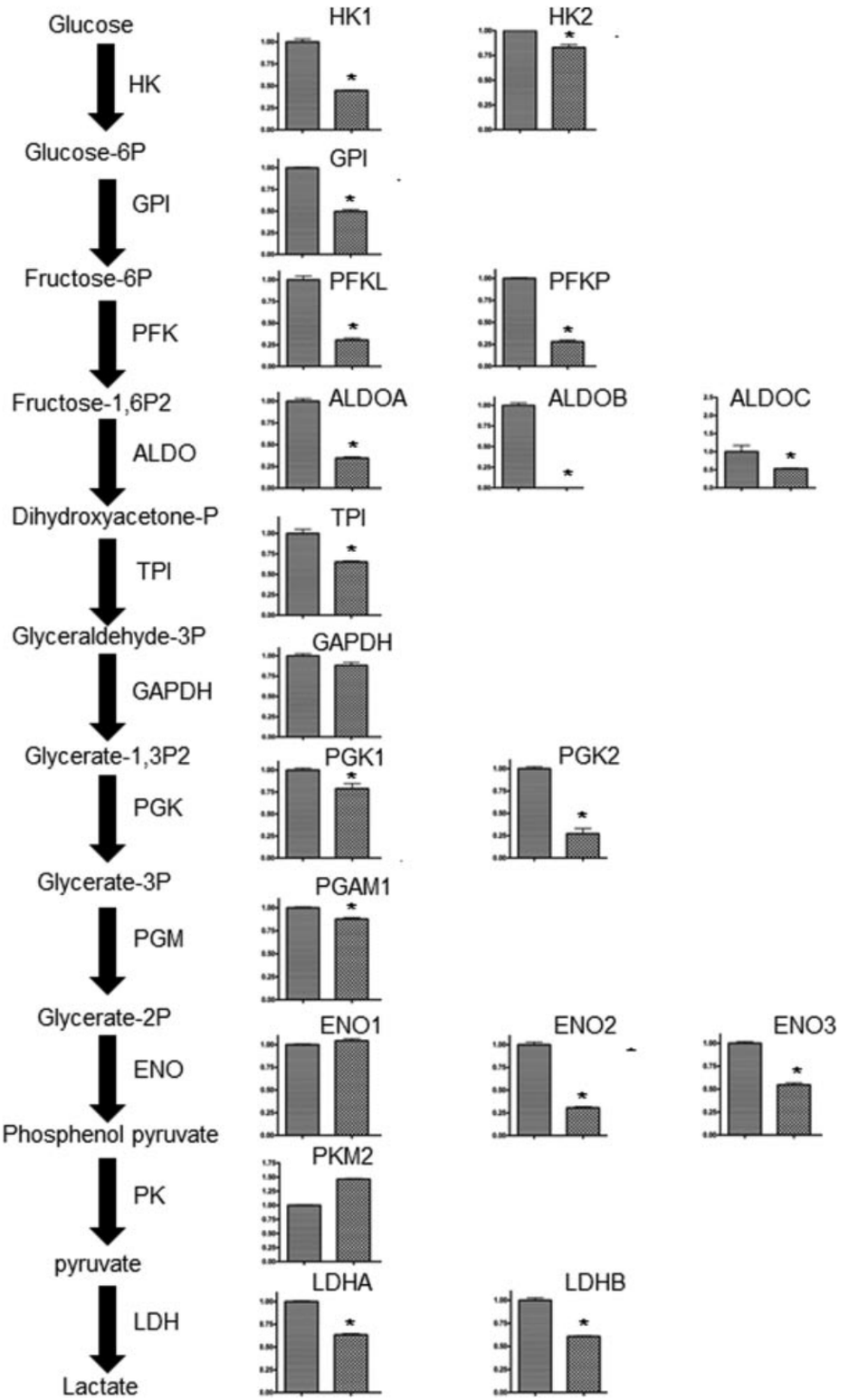

Figure 5. Effect of HNF-1β suppression on glycolytic enzymes Messenger RNA expression of *HK1*, *HK2*, *GPI*, *PFK-L*, *PFK-P*, *ALD-A*, *ALD-B*, *ALDOC*, *TPI*, *PGK1*, *PGK2*, *PGAM 1*, *ENO2*, *ENO3*, *LDHA*, and *LDHB* were decreased in RMG2-HNF1β-sh1 (right bar) cells, relative to RMG2-control cells (left bar). *HK*, hexokinase; *GPI*, glucose-6-phosphate isomerase; *PFK-L*, phosphofructokinase liver type; *PFK-P*, phosphofructokinase platelet type; *ALD*, aldolase; *TPI*, triosephosphate isomerase; *GAPDH*, glyceraldehyde-3-phosphate dehydrogenase; *PGK*, phosphoglycerate kinase; *PGAM*, phosphoglycerate mutase; *ENO*, enolase; *PKM*, pyruvate kinase muscle type; *LDH*, lactate dehydrogenase. $^{*}P < 0.05$. Experiments were done in duplicate.

the ability to distinguish OCCC from non-OCCC in both ovarian cancer cell line datasets and importantly, clinical ovarian cancer datasets (Figure 6C–E). These results support that HNF-1β plays a pivotal role in the biology of OCCC. In addition, a total of 23 genes including HNF-1β were overlapped between OCCC- and HNF-1β signature. Among them, eight genes (*ELOVL6*, *FXYD2*, *IVNS1ABP*, *LIPC*, *MED28*, *MITF*, *RELN*, *TNFAIP6*) have HNF-1 binding element (V$HNF1 01) by analyzing with GATHER software (http://gather.genome.duke.edu/). We also analyzed these 23 genes by DAVID software (http://david.abcc.ncifcrf.gov/), and found that genes belonging to GO slim terms related to cell proliferation and

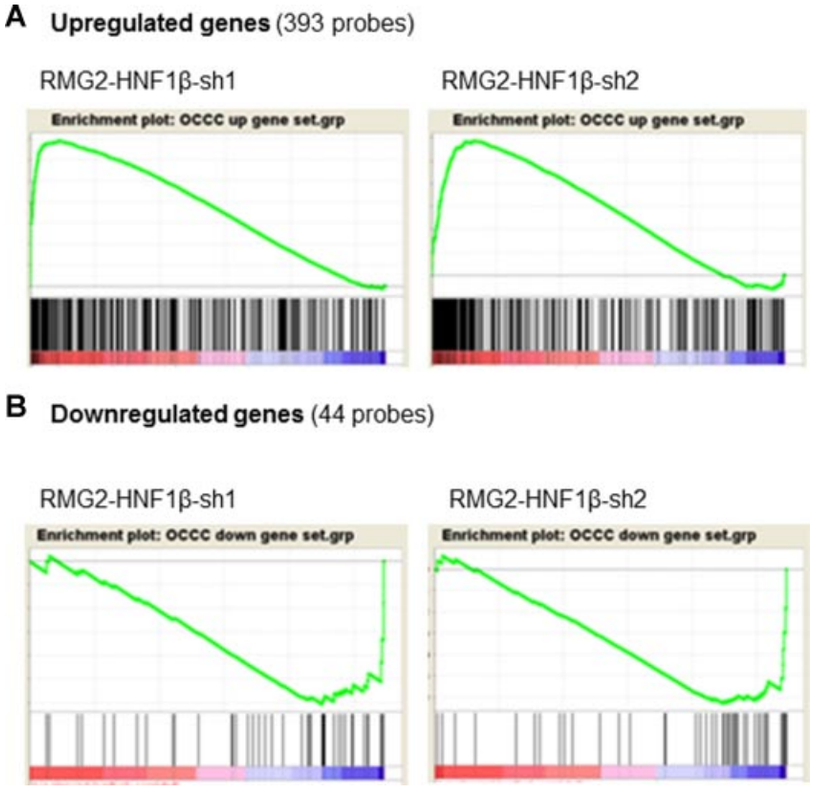

Figure 6. Gene expression microarray analysis showed that HNF-1β is a key molecule determining the OCCC gene expression profile. (A and B) Gene Set Enrichment Analysis. The *x*-axis represents rank of genes comprising of a particular gene set (signature genes) among the whole genes in the genome. Each vertical black line represents on signature genes, and the degree to which the black lines are deviated to the left or right indicates the statistical significance regarding increased expression of the signature genes in a particular group of samples (designated as enrichment). The *y*-axis represents Enrichment Score (ES) of the individual signature genes. Shift of the green line curve to the upper left indicates enrichment in the left, and shift to the lower right indicates enrichment in the right. (A) Left *x*-axis; Individual upregulated genes within the OCCC signature are shown as vertical black lines to see their deviation compared to the whole genes in the genome between the left (control shRNA samples, $n = 10$) and the right (HNF1β-sh1, $n = 5$). The genes comprising of this gene set were shifted to the left, which indicates enrichment in the RMG2-control-sh samples as compared to RMG2-HNF1β-sh1 samples (FDRq-value < 0.0001). (A) Right; Similarly, the upregulated genes within the OCCC signature were enriched in the RMG2-control-sh samples ($n = 10$) as compared to the RMG2-HNF1β-sh2 samples ($n = 5$) (FDRq-value < 0.0001). (B) The downregulated genes within the OCCC signature were significantly enriched in RMG2-HNF1β-sh1 and RMG2-HNF1β-sh2 cells as compared with RMG2-control cells (FDRq-value $= 0.0019$ and 0.0051, respectively). (C) Analysis using Bayesian binary regression. The HNF-1β signature was generated from 250 probe sets shown in each row. Red to blue indicates high to low expression. Each column represents an individual cell line. Ten columns on the left side represent shRNAs (both RMG2-HNF1β-sh1 and RMG2-HNF1β-sh2 cells) and the ten columns on the right side represent RMG2-control cells. (D) Leave-one-out cross-validation of training sets (RMG2-HNF1β-sh1 and RMG2-HNF1β-sh2 cells versus RMG2-control) using the HNF-1β signature genes. Blue and red colors indicate RMG2-HNF1β-sh cells ($n = 10$) and RMG2-control cells ($n = 10$), respectively. The probability estimates based on the HNF-1β signature genes is shown on the vertical axis with 95% confidence intervals. (E) OCCC has a higher probability of having the HNF-1β signature profile than non-OCCC. GSE6008 (0.93 ± 0.038 vs. 0.42 ± 0.21, $P < 0.0001$); GSE2109 (0.63 ± 0.30 vs. 0.48 ± 0.22, $P = 0.0112$); KyotoOv (0.61 ± 0.20 vs. 0.41 ± 0.22, $P = 0.012$). (F) The expression of *SOD1* gene (probe ID: 200642_at) is significantly decreased in RMG2-HNF1β-sh1 and RMG2-HNF1β-sh2 cells as compared to control cells ($P < 0.0001$ and $P = 0.0002$, respectively). (G) The validation of *SOD1* gene expression by qRT-PCR. RMG2-HNF1β-sh1 and RMG2-HNF1β-sh2 cells versus RMG2-control cells ($P = 0.0012$ and $P = 0.0001$, respectively). RMG1-HNF1β-sh1 versus RMG1-control cells ($P = 0.029$). RMG2-sh1, RMG2-HNF1β-sh1; RMG2-sh2, RMG2-HNF1β-sh2; RMG1-sh1, RMG1-HNF1β-sh1. $^{*}P < 0.05$.

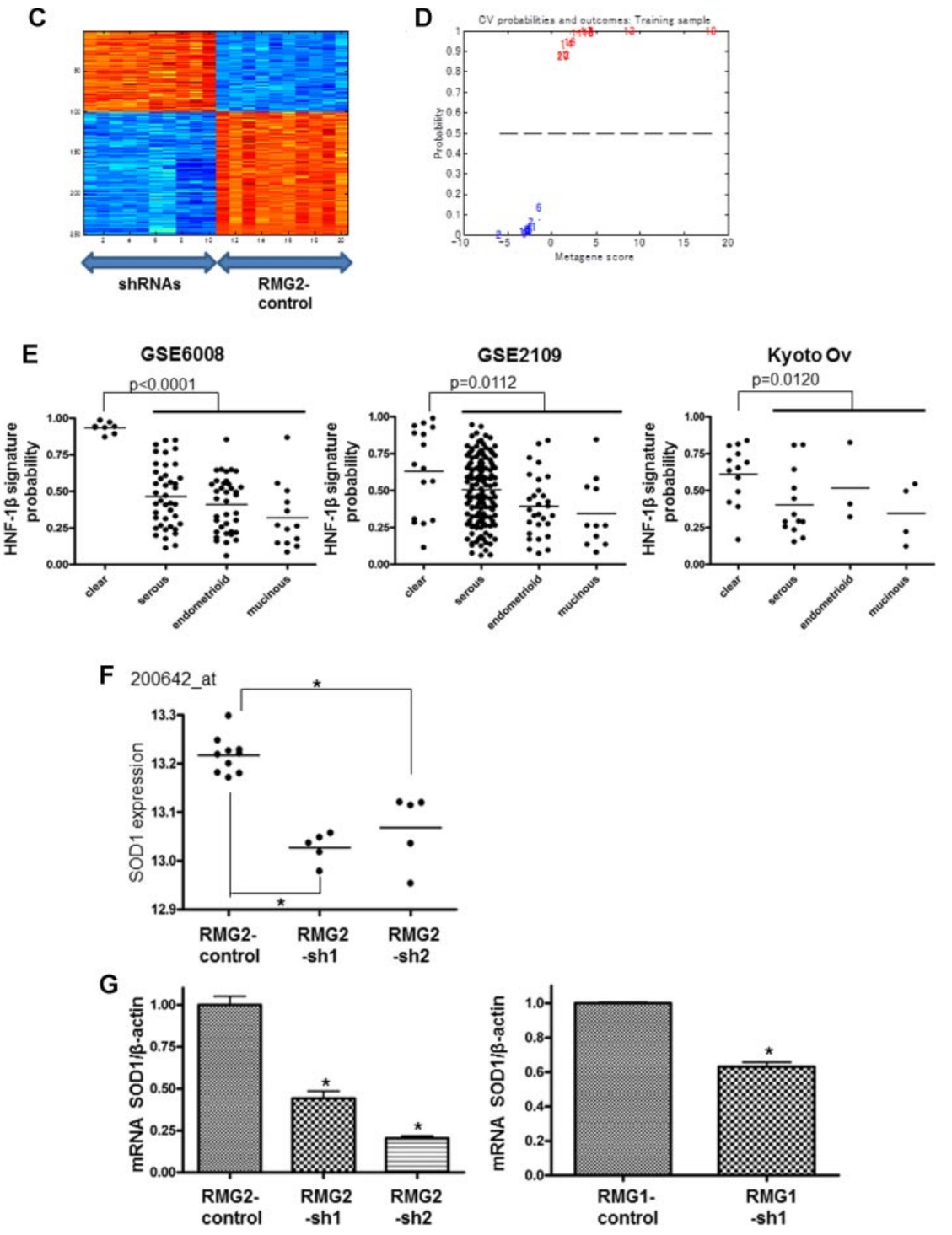

Figure 6. (*Continued*)

metabolism such as "negative regulation of cell proliferation ($P = 0.09$)," "carbohydrate binding ($P = 0.062$)," and "regulation of cellar response to stress ($P = 0.009$)" were enriched in these 23 genes.

Then, we tested if HNF-1β suppression affects cell proliferation and notably found that this significantly increases the growth rate of RMG2 cells. Moreover, transfection of the *HNF-1β* gene into Hey, a serous

ovarian cancer cell line with minimal HNF-1β expression, caused cell growth to be significantly decreased. These data suggest that HNF-1β functions as a suppressive regulator of cell proliferation. We then evaluated whether HNF-1β suppression causes leads to altered expression of the cell cycle regulator, CDKN1A and CDKN1B, and found that it causes marked reduction of CDKN1A and CDKN1B levels, suggesting that HNF-1β negatively controls cell proliferation by inducing expression of a potent cell cycle regulatory gene that inhibits G1 progression. As shown in Supplementary Table 4, *CDKN1B* has HNF-1 binding motif according to TRANSFAC dataset [21]. The cell cycle analysis using flow cytometry also suggests that HNF-1β act as inhibitor of cell cycle progression. Suppression of HNF-1β significantly increased cell population in S-phase. Taken together, observation of clinical cases as well as ovarian cancer cell lines indicates that OCCC generally grows slower than serous adenocarcinoma, which may partly be ascribed to the overexpression of HNF-1β in OCCC [3].

It is well documented that cancer cells exhibit unusually active metabolic processes when compared with normal cells. This "metabolic switch" in cancer cells is most prominent with regard to glucose metabolism [22–24]. In this study, we incidentally noticed that the culture media over time retained its red coloration from the phenol red (which is indicative of a more basic pH levels) in spite of the increased growth rate of the HNF-1β-knockdown RMG2 cells, suggesting that these cells may be secreting less lactate into the media. Indeed, measurement of lactate indicated that both RMG2-HNF1β-sh1 and RMG2-HNF1β-sh2 show significantly less efflux of lactate when compared with the RMG2-control. We then evaluated glucose uptake in these cells and found that it is also significantly lower in RMG2-HNF1β-sh1 and RMG2-HNF1β-sh2 cells than in the RMG2-control cells. Expression of the glucose transporter *GLUT1* mRNA as well as GLUT1 protein was found to be lower in RMG2-HNF1β-sh1 and RMG2-HNF1β-sh2 than in the RMG2-control cells. Conversely, forced expression of HNF-1β in Hey cells increased glucose uptake as well as expression of GLUT1. Furthermore, the observed significant reduction in glucose uptake in RMG2 cells following GLUT1 knockdown confirmed a major role of GLUT1 in mediating glucose transport in these cells (Supplementary Figure 1). In addition, *GLUT1* had HNF-1 binding motif according to TRANSFAC dataset provided by Jeffrey T. et al. (2006) [21] (Supplementary Table 4). These data suggest that HNF-1β increases glucose uptake at least in part by upregulating a glucose transporter gene.

We further evaluated the role of HNF-1β in glucose metabolism using an assay that measures glycolytic flux within cells. Knockdown of HNF-1β in RMG2 cells decreased the glycolytic flux rate in comparison with the control cells, while forced expression of HNF-1β in Hey cells had the opposite effect, suggesting that HNF-1β not only increases glucose uptake but also promotes glycolysis in cancer cells. In fact, further evaluation of gene expression related to the enzymatic activity associated with the glycolytic process revealed that a majority of the genes examined were repressed by HNF-1β knockdown. As shown in Supplementary Table 4, some of these glycolytic enzymes have HNF-1 binding motif according to TRANSFAC dataset [21]. It has been reported that activation of HIF-1α causes upregulation of GLUT1, glucose uptake, and glycolysis under hypoxic conditions [25–27]. Stany et al. [28] also showed that HIF-α pathway was activated as one of specific signaling pathways related to glucose metabolism in OCCC compared with those in high-grade serous ovarian cancer. HIF-1α protein is regulated at the posttranslational level via the ubiquitin-proteasome system under normoxic condition. In this study, we found that HNF-1β did not alter either mRNA or protein expressions of HIF-1α (Supplementary Figure 3). Therefore, HNF-1β is not likely to affect transcriptional or posttranscriptional levels of HIF-1α protein. On the other hand, HIF-2α is highly homologous and has similar binding motif as HIF-1α [29]. Therefore, we cannot exclude the possibility that HNF-1β might regulate the glycolytic pathway through HIF-2α.

The characteristically high glycolytic rate in cancer cells was first described by Otto Warburg and is referred to as the "Warburg effect" [30]. According to Warburg's observations, unlike normal tissue cells, cancer cells use glycolysis instead of using mitochondrial oxidative phosphorylation to obtain ATP, which leads to high glucose consumption and lactate production. Although not completely understood, it is presumed that this mechanism is used to meet the metabolic requirements to support rapid proliferation of cancer cells. Indeed, a similar metabolic switch is sometimes observed in normal physiological processes, such as embryonic development, wound healing, or immune reactions during which rapid cell proliferation is required [22]. In cancer cells, some oncogenic alterations have been shown to evoke the Warburg effect [31–34]. In this study, for the first time, we demonstrated that an important function of HNF-1β is to promote the glycolytic process, namely the Warburg effect.

The reason why HNF-1β functions in this manner in OCCC is yet to be elucidated. However, it is noteworthy that this study also found that HNF-1β suppresses cell proliferation along with promoting glycolysis. Hence, increased glycolytic metabolism does not occur in parallel to increased cell proliferation with regard to HNF-1β function, similar to the case of many oncogenes [35]. These findings may indicate that the reasons for overexpression of HNF-1β in OCCC may not necessarily be to meet energy requirements for cell proliferation. Inversely, serous ovarian cancer, typically more rapidly growing

tumors than OCCC, seldom show HNF-1β overexpression. Recently, elevated glycolytic rates have been shown to contribute to the inhibition of oxidative stress-induced apoptosis in cancer cells as well as in normal cells, under some conditions [36,37]. We have shown that OCCC arises in the extraordinarily stressful environment of oxygen free radical-enriched endometriotic cysts and expresses significantly more stress-related genes as compared to other histologic types of epithelial ovarian cancers [8]. In this context, HNF-1β may act as a stress-reducer that allows for survival of OCCC cells, although further study is needed to test this hypothesis.

ACKNOWLEDGMENTS

The experiments using radioisotope were performed in the Radioisotope Research Center of Kyoto University and Timothy Haystead's Laboratory of Duke University with helpful assistance from the staff. We also gratefully acknowledge the excellent technical assistance of Yuko Hosoe and Maki Kurokawa.

REFERENCES

1. Mandai M, Yamaguchi K, Matsumura N, Baba T, Konishi I. Ovarian cancer in endometriosis: Molecular biology, pathology, and clinical management. Int J Clin Oncol 2009;14:383–391.
2. Kobayashi H. Ovarian cancer in endometriosis: Epidemiology, natural history, and clinical diagnosis. Int J Clin Oncol 2009;14:378–382.
3. Itamochi H, Kigawa J, Terakawa N. Mechanisms of chemoresistance and poor prognosis in ovarian clear cell carcinoma. Cancer Sci 2008;99:653–658.
4. Kobayashi H, Sumimoto K, Moniwa N, et al. Risk of developing ovarian cancer among women with ovarian endometrioma: A cohort study in Shizuoka, Japan. Int J Gynecol Cancer 2007;17:37–43.
5. Sugiyama T, Kamura T, Kigawa J, et al. Clinical characteristics of clear cell carcinoma of the ovary: A distinct histologic type with poor prognosis and resistance to platinum-based chemotherapy. Cancer 2000;88:2584–2589.
6. Goff BA, Sainz de la Cuesta R, Muntz HG, et al. Clear cell carcinoma of the ovary: A distinct histologic type with poor prognosis and resistance to platinum-based chemotherapy in stage III disease. Gynecol Oncol 1996;60:412–417.
7. Yamaguchi K, Mandai M, Toyokuni S, et al. Contents of endometriotic cysts, especially the high concentration of free iron, are a possible cause of carcinogenesis in the cysts through the iron-induced persistent oxidative stress. Clin Cancer Res 2008;14:32–40.
8. Yamaguchi K, Mandai M, Oura T, et al. Identification of an ovarian clear cell carcinoma gene signature that reflects inherent disease biology and the carcinogenic processes. Oncogene 2010;29:1741–1752.
9. Bach I, Mattei MG, Cereghini S, Yaniv M. Two members of an HNF1 homeoprotein family are expressed in human liver. Nucleic Acids Res 1991;19:3553–3559.
10. Bingham C, Hattersley AT. Renal cysts and diabetes syndrome resulting from mutations in hepatocyte nuclear factor-1beta. Nephrol Dial Transplant 2004;19:2703–2708.
11. Maestro MA, Cardalda C, Boj SF, Luco RF, Servitja JM, Ferrer J. Distinct roles of HNF1beta, HNF1alpha, and HNF4alpha in regulating pancreas development, beta-cell function and growth. Endocr Dev 2007;12:33–45.
12. Tsuchiya A, Sakamoto M, Yasuda J, et al. Expression profiling in ovarian clear cell carcinoma: Identification of hepatocyte nuclear factor-1 beta as a molecular marker and a possible molecular target for therapy of ovarian clear cell carcinoma. Am J Pathol 2003;163:2503–2512.
13. Matsumura N, Mandai M, Okamoto T, et al. Sorafenib efficacy in ovarian clear cell carcinoma revealed by transcriptome profiling. Cancer Sci 2010;101:2658–2663.
14. Wakasugi M, Matsuura K, Nagasawa A, et al. DDB1 gene disruption causes a severe growth defect and apoptosis in chicken DT40 cells. Biochem Biophys Res Commun 2007;364:771–777.
15. Shi DY, Xie FZ, Zhai C, Stern JS, Liu Y, Liu SL. The role of cellular oxidative stress in regulating glycolysis energy metabolism in hepatoma cells. Mol Cancer 2009;8:32.
16. Kondoh H, Lleonart ME, Gil J, et al. Glycolytic enzymes can modulate cellular life span. Cancer Res 2005;65:177–185.
17. Kato N, Toukairin M, Asanuma I, Motoyama T. Immunocytochemistry for hepatocyte nuclear factor-1beta (HNF-1beta): A marker for ovarian clear cell carcinoma. Diagn Cytopathol 2007;35:193–197.
18. Kao YC, Lin MC, Lin WC, Jeng YM, Mao TL. Utility of hepatocyte nuclear factor-1beta as a diagnostic marker in ovarian carcinomas with clear cells. Histopathology 2012;61:760–768.
19. Fadare O, Liang SX. Diagnostic utility of hepatocyte nuclear factor 1-beta immunoreactivity in endometrial carcinomas: Lack of specificity for endometrial clear cell carcinoma. Appl Immunohistochem Mol Morphol 2012;20:580–587.
20. Kato N, Tamura G, Motoyama T. Hypomethylation of hepatocyte nuclear factor-1beta (HNF-1beta) CpG island in clear cell carcinoma of the ovary. Virchows Arch 2008;452:175–180.
21. Chang JT, Nevins JR. GATHER: A systems approach to interpreting genomic signatures. Bioinformatics 2006;22:2926–2933.
22. Levine AJ, Puzio-Kuter AM. The control of the metabolic switch in cancers by oncogenes and tumor suppressor genes. Science 2010;330:1340–1344.
23. Mentis AF, Kararizou E. Metabolism and cancer: An up-to-date review of a mutual connection. Asian Pac J Cancer Prev 2010;11:1437–1444.
24. DeBerardinis RJ. Is cancer a disease of abnormal cellular metabolism? New angles on an old idea. Genet Med 2008;10:767–777.
25. Marin-Hernandez A, Gallardo-Perez JC, Ralph SJ, Rodriguez-Enriquez S, Moreno-Sanchez R. HIF-1alpha modulates energy metabolism in cancer cells by inducing over-expression of specific glycolytic isoforms. Mini Rev Med Chem 2009;9:1084–1101.
26. Gillies RJ, Gatenby RA. Adaptive landscapes and emergent phenotypes: Why do cancers have high glycolysis? J Bioenerg Biomembr 2007;39:251–257.
27. Semenza GL. HIF-1 mediates the Warburg effect in clear cell renal carcinoma. J Bioenerg Biomembr 2007;39:231–234.
28. Stany MP, Vathipadiekal V, Ozbun L, et al. Identification of novel therapeutic targets in microdissected clear cell ovarian cancers. PLoS ONE 2011;6:e21121.25.
29. Li Z, Bao S, Wu Q, et al. Hypoxia-inducible factors regulate tumorigenic capacity of glioma stem cells. Cancer Cell 2009;15:501–513.
30. Warburg O. On the origin of cancer cells. Science 1956;123:309–314.
31. Maddocks OD, Vousden KH. Metabolic regulation by p53. J M l Med 2011;89:237–245.
32. Kondoh H. Cellular life span and the Warburg effect. Exp Cell Res 2008;314:1923–1928.
33. Dang CV, Le A, Gao P. MYC-induced cancer cell energy metabolism and therapeutic opportunities. Clin Cancer Res 2009;15:6479–6483.

34. Yeung SJ, Pan J, Lee MH. Roles of p53, MYC and HIF-1 in regulating glycolysis—The seventh hallmark of cancer. Cell Mol Life Sci 2008;65:3981–3999.
35. Fritz V, Fajas L. Metabolism and proliferation share common regulatory pathways in cancer cells. Oncogene 2010;29: 4369–4377.
36. Kondoh H, Lleonart ME, Bernard D, Gil J. Protection from oxidative stress by enhanced glycolysis; a possible mechanism of cellular immortalization. Histol Histopathol 2007;22: 85–90.
37. Ruckenstuhl C, Buttner S, Carmona-Gutierrez D, et al. The Warburg effect suppresses oxidative stress induced apoptosis in a yeast model for cancer. PLoS ONE 2009;4:e4592.

SUPPORTING INFORMATION

Additional supporting information may be found in the online version of this article at the publisher's web-site.